Use of simple models to estimate effect of density on fracture behaviour of sintered steel

N. A. Fleck and R. A. Smith

Two material models are developed to estimate the effect of density on the static and cyclic fracture behaviour of a sintered steel. The models are based on the known micromechanisms of failure for each type of loading. Theoretical predictions are compared with previous experimental results taken from a companion paper (preceding). The two models successfully account for the variation of yield stress, ultimate tensile stress, and fracture toughness with density. They prove less successful in predicting the effect of density on fatigue crack propagation behaviour. PM/0198

 Manuscript received 7 December 1980; in final form 1 April 1981. The authors are in the Engineering Department, University of Cambridge.

LIST OF SYMBOLS

a	crack length
A_n	nominal area of section
A_t	load-bearing area of section
E	Young's modulus
K_C	fracture toughness
K_{1C}	plane-strain fracture toughness
ΔK	stress-intensity factor range
ΔK_0	stress-intensity factor range corresponding to a growth rate of 10^{-9} m/cycle
ΔK_{th}	threshold stress-intensity factor range
N	number of fatigue cycles
$P=\frac{\rho_0-\rho}{\rho_0}$	fractional porosity
R_A	centreline average roughness value
S	inclusion spacing
ϵ_f	true failure strain
σ_n	nominal tensile stress on section
σ_t	tensile stress experienced by interparticle necks
σ_{UTS}	ultimate tensile strength
σ_y	0·2% offset yield stress
ρ	density
ρ_0	full density
$\lambda, \chi_{V,B}$	non-dimensional parameters

The mechanical properties of sintered steel depend upon many variables. These include chemical composition, origin of powder, sintering conditions, and any subsequent thermal or mechanical treatments. One variable which is easily controlled by the sintered-component manufacturer and which has a dramatic effect upon mechanical properties is the density of compact.

The pores within a sintered steel are known to reduce the net load-bearing section and to exert a stress concentrating influence.[1-3] Any material model must take these into account together with the correct micromechanism of failure. The micromechanism of failure depends upon such variables as the composition of the steel, and the type of loading imposed.[2,4-6] Several workers[7-9] have attempted to relate properties such as the fatigue limit to the metallographic structure and tensile properties. Few, however, have looked at the role of microstructure in cyclic and static cracking from a fracture mechanics viewpoint.

In a related paper,[10] the effect of density upon the tensile strength, fracture toughness, and resistance to fatigue crack propagation of a sintered steel was experimentally investigated. In this paper the authors seek to develop a material model which can account for these experimental observations.

PREVIOUS EXPERIMENTAL WORK

The effect of a variation in density upon the 0·2% offset yield stress, ultimate tensile stress, resistance to fatigue crack propagation, and fracture toughness of a sintered steel was investigated. The steel chosen for study was of composition Fe–1·5Cu–1·75Ni–0·50Mo–0·50C; density was varied from 6580 to 6980 kg m^{-3}. The steel compacts were sintered for 30 min at 1150°C in an atmosphere of cracked ammonia; *see* Ref. 10 for details.

THEORETICAL MATERIAL MODELS

Many theoretical, empirical, and semiempirical models have been developed to describe the tensile behaviour of sintered materials.[3,11,12] To be successful the models must be based on the correct micromechanism of failure, and take into account both porosity level and pore geometry.

Two idealizations are discussed: the variable morphology model by Griffiths *et al.*,[13] and a simple brick model, developed by the authors. The fully developed forms of these two models are based on the following assumptions:

(i) failure due to tensile loading, static and cyclic cracking occurs by the process of microvoid coalescence in the necks, between sintered steel particles

(ii) the stress state at the tip of a static or cyclic crack is closer to plane stress than to plane strain, for any thickness of testpiece

(iii) the stress σ_t experienced by the necks is greater than the stress σ_n imposed on the section by a factor $(1/\chi_{V,B})$ where $\chi_{V,B}$ is a non-dimensional parameter $(0 \leqslant \chi_{V,B} \leqslant 1)$.

(iv) a static or cyclic crack propagates through those necks closest to the crack tip, i.e. without jumping to more distant necks.

Assumption (i) is shown to be valid from previous experi-

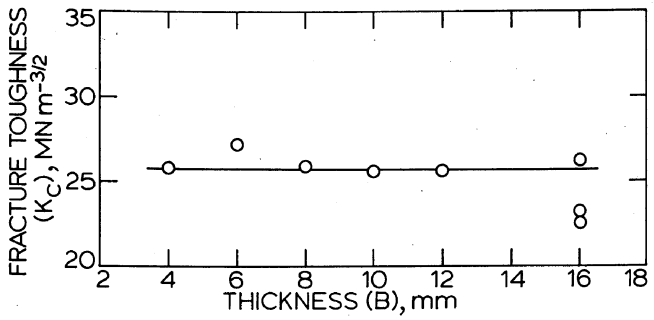

1 Effect of specimen thickness on measured fracture toughness: ρ=6810 kg m^{-3}

mental work.[10] Firm evidence for assumption (ii) is given in Fig. 1, where the measured fracture toughness of three-point bend specimens is plotted against thickness of test-piece. Each data point represents one test result, at a density of 6810 kg m^{-3}. The ASTM standard E399–78[14] stipulates a minimum thickness requirement of $2{\cdot}5(K_{1C}/\sigma_y)^2$ for plane-strain conditions at the crack tip. This gives a minimum thickness of 16 mm, for a plane-strain fracture toughness K_{1C} of 24 MN m$^{-3/2}$ and a yield stress σ_y of 300 MN m^{-2}. It is clear from Fig. 1 that fracture toughness is invariant with thickness for thicknesses much less than the minimum thickness requirement, and so there is no transition from plane stress to plane strain. It is concluded that the stress state at the crack tip is closer to plane stress than to plane strain, regardless of specimen thickness. Thus the elastic–plastic techniques employed by Crane and Farrow[15] to characterize the fracture toughness of the same material are unnecessary.

Assumption (iii) is discussed below, where it is shown that the term $X_{V,B}$ is a function of both porosity level and pore geometry. Confirmation for assumption (iv) is found from a fractographic investigation carried out on failed specimens, using the scanning electron microscope.[10] The variation in height of fracture surface from one failed particle to the next was always less than the maximum particle size of 230 μm. This was true for all types of loading. Surface roughness measurements carried out on the fracture surfaces further showed that:

(i) the variation in height from one failed particle to the next was always less than 100 μm, the mean particle size

(ii) the centreline average roughness value R_A was 21 ± 3 μm for all densities and modes of failure.

It is concluded that the crack keeps in-plane within the particle size limits, i.e. ± 50 μm.

From the basis of the above assumptions, the two material models can be developed to account for the variation of tensile strength, resistance to fatigue crack propagation, and fracture toughness with density.

Variable morphology model

Griffiths *et al.*[13] have modelled the pores in a sintered steel to be a distribution of spheres and oblate ellipsoids. They found that the tensile strength $(\sigma_{UTS})_\rho$ of a porous material varied with fractional porosity $P(=\rho_0-\rho/\rho_0)$ according to

$$\frac{(\sigma_{UTS})_\rho}{(\sigma_{UTS})_{\rho_0}} = 1-\lambda P^{2/3} \quad \ldots\ldots\ldots\ldots\ldots\ldots (1)$$

where $(\sigma_{UTS})_{\rho_0}$ is the tensile strength of the fully dense material, and λ is a function of pore geometry. The model gave different values for λ according to the major/minor diameter ratio of a typical pore. The sintered steel discussed previously[10] possessed a typical particle size of 100 μm, neck dia. of 20 μm, and local radius of curvature at the necks of 10 μm. This yields a value for λ of 1·66, which is in close agreement with the experimental value of 1·7 quoted by Ishimaru *et al.*,[16] for a sintered steel of similar composition.

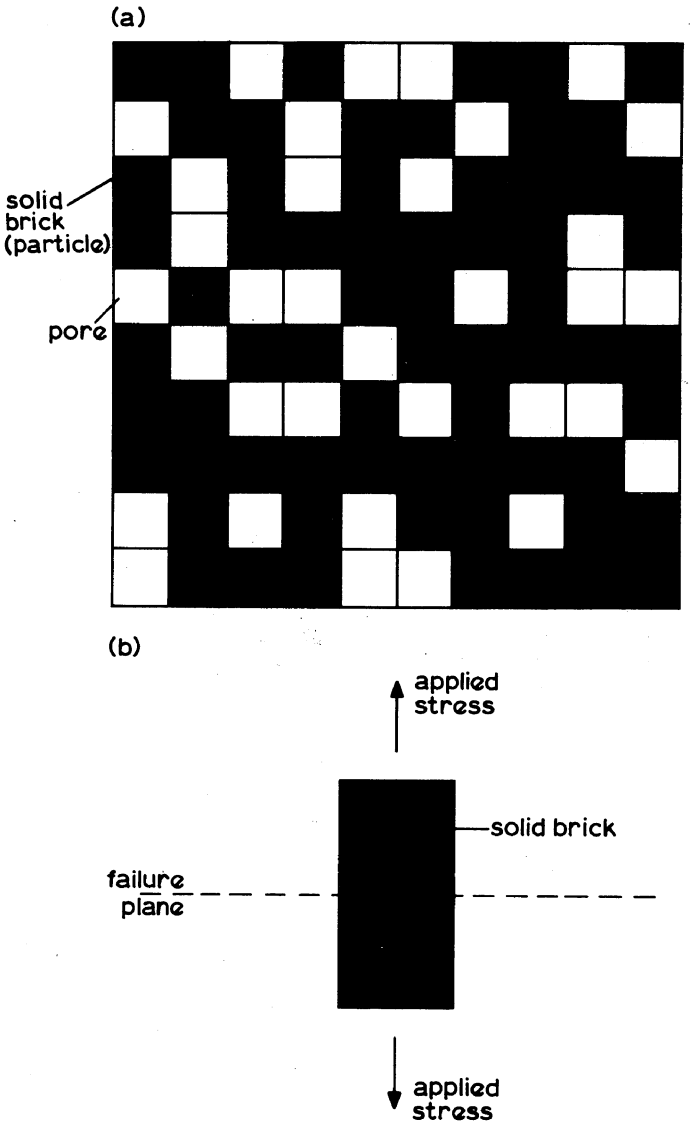

2 *a* typical section of simple brick model, probability of pore=$P^{2/3}$, probability of solid brick=$1-P^{2/3}$; *b* mode of failure of simple brick model, probability of failure plane lying between two solid bricks=$(1-P^{2/3})^2$

Simple brick model

The pores and particles may alternatively be modelled as a layered randomly organized array of cubes. Particles are represented by solid cubes, pores by cubic spaces. The stress concentrating effects due to pore geometry are ignored. A typical section through the sintered steel is idealized in Fig. 2*a*.

The probability of a pore existing at any location is given by $P^{2/3}$, while the probability of the existence of a brick is $1-P^{2/3}$. Thus the probability of the failure plane lying between two solid bricks is $(1-P^{2/3})^2$ (Fig. 2*b*). The strength $(\sigma_{UTS})_\rho$ of the sintered material is therefore proportional to $(1-P^{2/3})^2$, and we may write

$$\frac{(\sigma_{UTS})_\rho}{(\sigma_{UTS})_{\rho_0}} = (1-P^{2/3})^2 \quad \ldots\ldots\ldots\ldots\ldots\ldots (2)$$

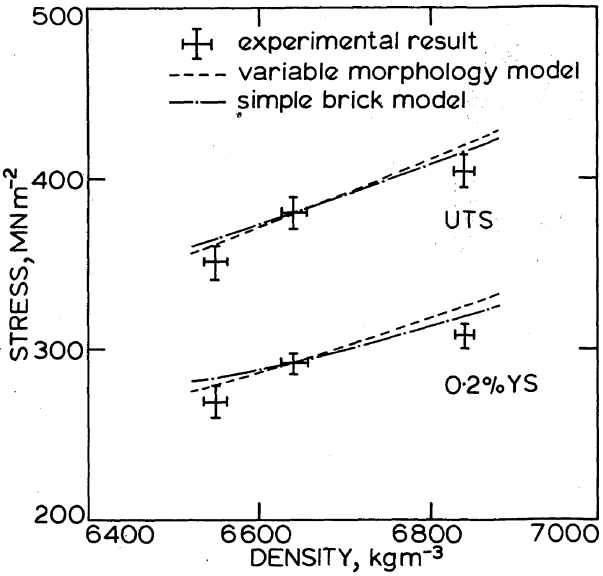

3 Effect of density on ultimate tensile stress (UTS) and yield stress (0·2% YS)

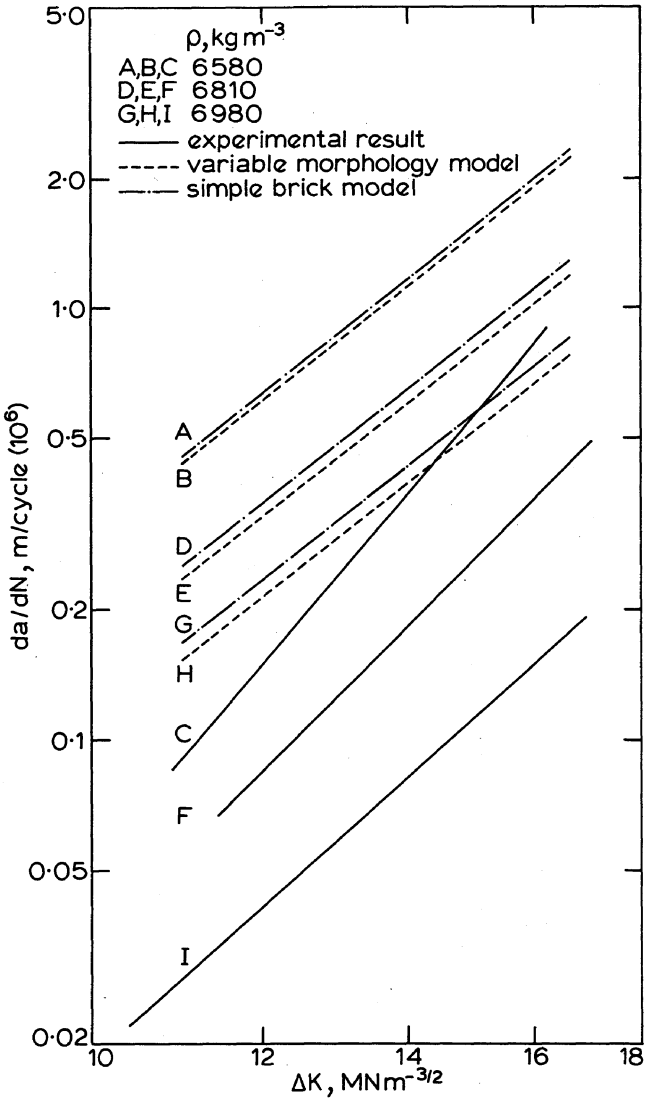

4 Effect of density on fatigue crack propagation behaviour

Now assumption (iv) was that the tip of a static or cyclic crack is unable to jump by more than one particle size and so there is no need to consider further probability terms in equation (2). In agreement with assumption (i) the model uses an interparticle type of fracture.

The variable morphology and simple brick models may now be developed to give expressions for the variation of yield stress, resistance to fatigue crack propagation, and fracture toughness with density.

Tensile behaviour

Several investigators[17,18] have shown that the ratio $(\sigma_{UTS})_\rho / (\sigma_{UTS})_{\rho_0}$ is equal to the ratio of load-bearing section A_t divided by the nominal section A_n. This ratio will subsequently be noted by $\chi_{V,B}$ where the subscript V refers to the variable morphology model, the subscript B to the simple brick model. The load-bearing section A_t may be further identified with the area of necks projected on to any section; the stress σ_t experienced by the necks is therefore related to nominal tensile stress σ_n by

$$\frac{\sigma_n}{\sigma_t} = \frac{A_t}{A_n} = \frac{(\sigma_{UTS})_\rho}{(\sigma_{UTS})_{\rho_0}} = \chi_{V,B} \quad \ldots\ldots\ldots\ldots (3)$$

where

$$\chi_V = 1 - \lambda P^{2/3} \quad \ldots\ldots\ldots\ldots\ldots\ldots (4)$$

$$\chi_B = (1 - P^{2/3})^2 \quad \ldots\ldots\ldots\ldots\ldots\ldots (5)$$

For the sintered steel considered, λ is given the value of 1·7.[16]

It is expected that the yield stress $(\sigma_y)_\rho$ varies with density in the same manner as ultimate tensile stress $(\sigma_{UTS})_\rho$; hence

$$\frac{(\sigma_y)_\rho}{(\sigma_y)_{\rho_0}} = \chi_{V,B} \quad \ldots\ldots\ldots\ldots\ldots\ldots (6)$$

from equation (3). The term $(\sigma_y)_{\rho_0}$ denotes the yield stress of fully dense material.

Fatigue crack propagation behaviour

Various equations have been proposed to model the fatigue crack propagation behaviour of a fully dense material in terms of its monotonic tensile properties.[19] For the sintered steel investigated,[10] cyclic crack advance occurs mainly by microvoid coalescence in the necks between steel particles. Ashby[19] has developed a model to predict the crack growth rate for such a failure mechanism

$$\frac{da}{dN} \simeq \frac{\Delta K^4}{4\pi^2 \sigma_y^2 E^2 \epsilon_f^2 S} \quad \ldots\ldots\ldots\ldots\ldots\ldots (7)$$

From equation (7), the crack growth rate da/dN is related to the stress-intensity factor range ΔK, monotonic yield stress σ_y, Young's modulus E, failure strain ϵ_f, and inclusion spacing S. The model was derived for the fully dense material; it will now be modified to account for the effects of porosity.

Since the stress σ_t experienced by the sintered steel necks is greater than the nominal section stress σ_n by a factor $1/\chi_{V,B}$, it is argued that the nominal stress-intensity factor range ΔK should be replaced by the term $(\Delta K/\chi_{V,B})$. The fatigue crack propagation rate is increased by a further factor (A_n/A_t) or $1/\chi_{V,B}$, since it is assumed that the fatigue crack propagates instantaneously through the pores. The fatigue crack propagation equation becomes

$$\frac{da}{dN} \simeq \frac{\Delta K^4}{4\pi^2 E^2 \sigma_y^2 \epsilon_f^2 S} \left(\frac{1}{\chi_{V,B}}\right)^5 \quad \ldots\ldots\ldots\ldots (8)$$

Fracture-toughness behaviour

Models have been developed[19] to estimate the fracture toughness K_C of a fully dense material in terms of its monotonic tensile properties. When failure occurs by a ductile

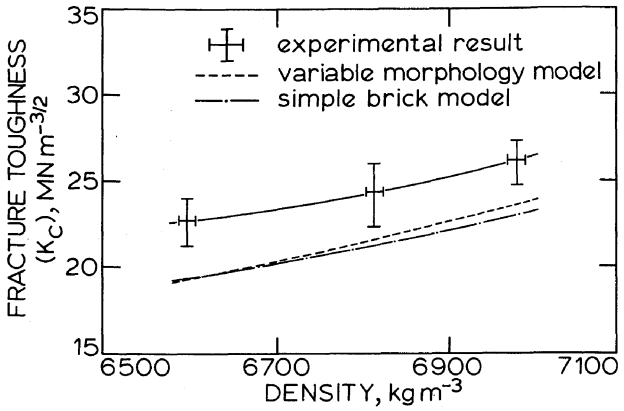

5 Effect of density on fracture toughness: thickness B=16 mm

tearing mechanism, with plane-stress conditions prevailing at the crack tip, assumption (ii), K_C may be modelled[19] by the equation

$$K_C \simeq \sqrt{2\pi\sigma_y E\epsilon_f S} \quad \ldots\ldots\ldots\ldots\ldots (9)$$

For the case of a porous material, equation (9) becomes

$$K_C \simeq \chi_{v,B}\sqrt{2\pi\sigma_y E\epsilon_f S} \quad \ldots\ldots\ldots\ldots\ldots (10)$$

since the true stress σ_t experienced by the necks is greater than the nominal stress σ_n by a factor of $1/\chi_{v,B}$.

COMPARISON OF MODELS WITH EXPERIMENTAL RESULTS

Before the material models can be used to estimate fracture behaviour, numerical values must be ascribed to the material constants E, σ_y, ϵ_f, and S in equations (8) and (10). These parameters relate to the fully dense material in the vicinity of the crack tip.[19]

The Young's modulus E is given the value 210 GN m^{-2}, typical of a low-alloy steel. Experimental investigation[10] shows the typical inclusion spacing S to be 2 μm. The depth of failed microvoid cusp is also of this order; hence a reasonable estimate of the failure strain ϵ_f is 1. A value for the yield stress of fully dense material $(\sigma_y)_{\rho 0}$ can be derived from equation (6) using the experimental result that the yield stress $(\sigma_y)_\rho$ at a density of 6640 kg m^{-3} is 294 MN m^{-2}. Accordingly, the variable morphology model and the simple brick model give $(\sigma_y)_{\rho 0}$ as 575 and 580 MN m^{-2} respectively. The ultimate tensile stress for the fully dense material $(\sigma_{UTS})_{\rho 0}$ can similarly be estimated.

Using these values in equations (3)–(6), (8), and (10) the results shown in Figs. 3–5 can be obtained. Also shown are experimental values taken from Ref. 10.

Tensile behaviour

Both models satisfactorily predict the increase in yield stress and ultimate tensile stress with increasing density (*see* Table 1 and Fig. 3). The discrepancy between estimated and experimental values is little more than the scatter in experimental results. Only the change in yield stress and ultimate tensile stress with density is of interest since equations (3) and (6) have been based on the experimental values at a density of 6640 kg m^{-3}.

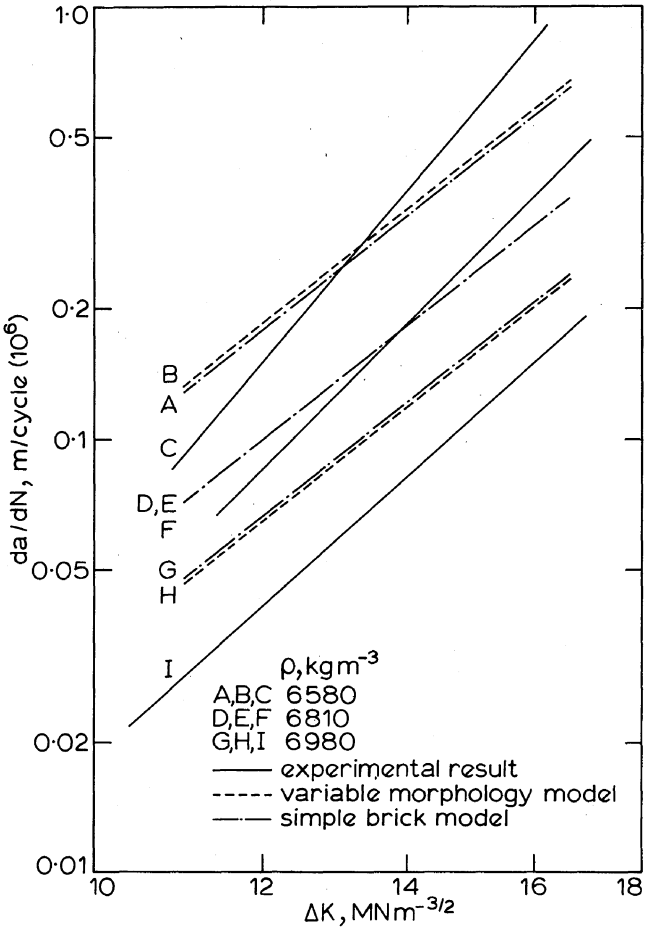

6 Effect of density on fatigue crack propagation behaviour: models have been adjusted to experimental results at ΔK=14 MN m$^{-3/2}$, ρ=6810 kg m^{-3}

Fatigue crack propagation behaviour

Both the experimental results and the two models show crack propagation rates to be very sensitive to changes in ΔK and density (Fig. 4). It was found experimentally that significant static tearing occurs alongside fatigue crack advance;[10] this may account for the observation that the measured slopes of the power law plot of da/dN *v.* ΔK are greater than the theoretical value of 4, as given by the two models.

The estimated crack growth rates are greater than the measured rates by a factor of 3–5. Since values for E, σ_y, ϵ_f, and S are not known exactly, and equations (7) and (8) are in any case approximate for the fully dense material, such a discrepancy is to be expected. It has been suggested[10,20,21]

Table 1 Effect of density on measured and estimated tensile strength and fracture toughness

Density range, kg m^{-3}	Change in density, %	Property	Corresponding range in property (with percentage change)		
			Measured	Variable morphology model	Simple brick model
6550–6840	4·4	Yield stress, MN m^{-2}	270–305 (11)	280–325 (16)	280–320 (14)
6550–6840	4·4	Ultimate tensile stress, MN m^{-2}	350–400 (15)	360–420 (16)	365–415 (14)
6580–6980	6·1	Fracture toughness, MN m$^{-3/2}$	22–26 (16)	19–24 (23)	19–23 (20)

that the pores may blunt the fatigue crack tip and so retard the crack propagation process. This would have the effect of depressing measured growth rates below the predicted values by some unknown factor.

In order to compare trends rather than absolute values, the theoretical predictions of both models are fitted to one experimental point. The point chosen is a stress-intensity factor range ΔK of 14 MN m$^{-3/2}$ and density ρ of 6810 kg m^{-3} (*see* Fig.6). The measured crack growth rates decrease by a factor of 3–5 when the density is increased from 6580 to 6980 kg m^{-3}. The variable morphology model predicts a corresponding decrease by a factor of 2·8, while the simple brick model predicts a decrease by a factor of 2·5. It is concluded that the models underestimate the effect of density upon growth rates. They do, however, go some way to account for the fatigue crack propagation behaviour of the sintered steel.

Fracture-toughness behaviour

Figure 5 and Table 1 show that the fracture-toughness behaviour of sintered steel is adequately described by the two models. When the density is increased from 6580 to 6980 kg m^{-3}, the measured fracture toughness increases by 16%, compared with 23% by the variable morphology model and 20% by the simple brick model.

Since equation (10) is only approximate and accurate values for E, σ_y, ϵ_f, and S are not known, exact predictions of the fracture toughness are not expected.

Barnby *et al.*[22] have found that the fracture toughness of sintered metals increases linearly with yield stress. Equations (6) and (10) show that the two models predict such behaviour.

It was suggested in the associated paper[10] that the pores neither sharpen nor blunt a crack at incipient static failure. Thus it is reasonable to use simple models which make no attempt to account for such blunting or sharpening, when investigating fracture-toughness behaviour.

CONCLUSIONS

Assuming a knowledge of the micromechanisms of failure under static and cyclic loading, two material models have been developed to estimate the variation with density of tensile strength, resistance to fatigue crack propagation, and fracture toughness of a sintered steel.

These models successfully account for the effect of density upon tensile and fracture-toughness properties. The models are less successful in predicting the effect of density upon fatigue crack propagation rates. This is partly due to the mixed static–cyclic failure mechanisms which operate in fatigue, but mainly to the inadequacy of present theoretical growth laws to quantitatively predict the performance of fully dense materials.

For the sintered steel investigated, a complex (variable morphology) model which accounts for pore geometry in addition to density is shown to be of limited value. A simpler (brick) model, which accounts only for density, predicts behaviour to comparable accuracy.

ACKNOWLEDGMENTS

One of the authors (NAF) is supported by a research studentship from the Department of Education, Northern Ireland. Both authors thank GKN Group Technological Centre for providing the testpieces.

REFERENCES

1. M. EUDIER: *Powder Metall.*, 1962, **6**, (9), 278.
2. R. HAYNES: *ibid.*, 1970, **13**, (26), 465.
3. H. E. EXNER and D. POHL: *Powder Metall. Int.*, 1978, **10**, (4), 193.
4. T. HONDA and Y. TOKUNAGA: *J. Jpn Soc. Powder Metall.*, 1976, **23**, 2, 10.
5. T. HONDA: *ibid.*, 1976, **23**, (2), 23.
6. P. FRANKLIN and B. L. DAVIES: *Powder Metall.*, 1978, **21**, 7.
7. I. KONDA and K. ŌKITA: *Powder Metall.*, 1972, **18**, 302.
8. H. H. HAUSNER, P. K. JOHNSON, and K. H. ROLL: 'Iron powder metallurgy', Pt III, 326; 1968, New York, Plenum Press.
9. M. MORITA, T. TAKAHASHI, and H. KISHIMOTO: *Toyota Eng.*, 1968, **15**, 107.
10. N. A. FLECK and R. A. SMITH: *Powder Metall.*, this issue, 121–125.
11. A. SALAK, V. MIŠKOVIĆ, E. DUDROVÁ, and E. RUDNAYOVA: *Powder Metall. Int.*, 1974, **6**, 123.
12. F. J. ESPER, H. E. EXNER, and H. METZLER: *Powder Metall.*, 1975, **18**, (35), 107.
13. T. J. GRIFFITHS, R. DAVIES, and M. B. BASSETT: *ibid.*, 1979, **22**, 119.
14. 'Standard test method for plane-strain fracture toughness of metallic materials', ASTM Standards, E339-78, 1978.
15. L. W. CRANE and R. J. FARROW: *Powder Metall.*, 1980, **23**, 198.
16. Y. ISHIMARU, Y. SAITO, and Y. NISHINO: 'Modern developments in powder metallurgy', (ed. H. H. Hausner), Vol. 4, 441; 1971, New York, Plenum Press.
17. H. METZLER: dissertation, Stuttgart University, West Germany, 1972.
18. R. T. DE HOFF and J. P. GILLARD: 'Modern developments in powder metallurgy', (ed. H. H. Hausner), Vol. 4, 281; 1971, New York, Plenum Press.
19. M. F. ASHBY: 'Fracture mechanics – Current status, future prospects', (ed. R. A. Smith); 1980, Oxford, Pergamon.
20. S. H. WILLIAMS and R. HAYNES: *Powder Metall.*, 1973, **16**, (32), 387.
21. J. M. WHEATLEY and G. C. SMITH: *ibid.*, 1963, **6**, (12), 141.
22. J. T. BARNBY, D. C. GHOSH, and K. DINSDALE: *ibid.*, 1973, **16**, (31), 55.